Supporting Information

Superhydrophobic Auxetic Metamaterials

Glen McHale, Andrew Alderson, Steven Armstrong, Shruti Mandhani, Mahya Meyari, Gary G. Wells, Emma Carter, Rodrigo Ledesma-Aguilar, Ciro Semprebon, and Kenneth E. Evans*

EXPERIMENTAL METHODS

SU-8 Based Physical Model for an Auxetic Bow-Tie Lattice.

To make the physical model the manufacturers data sheet for SU8-3035 permanent negative resist (Kayaku Advanced Materials, Inc.) was used as a basis for the process and modified for specific equipment. In a clean room environment, 3" silicon wafers are coated with a 500±10 nm oxide layer *via* plasma enhanced chemical vapor deposition STS Multiplex PECVD) to promote adhesion between the wafer and photoresist (Fig. S1a). To further enhance adhesion the wafer is then treated with hexamethyldisilazane (HMDS) for 10 minutes by keeping the wafer in a closed container with an open vial containing 2-3 drops of HMDS. The photoresist (MEGAPOSIT^{TM} SU8-3035, Kayaku Advanced Materials) is then spin coated onto the oxide coated silicon wafer: 500 rpm for 10 seconds with 100 rpm s^{-1} acceleration; 2000 rpm for 30 seconds with 300 rpm s^{-1}; then soft baked for 10 minutes at 95°C (Fig. S1b). The thickness of photo resist is measured as 62±1 μm using a stylus profilometer (DektakXT, Bruker). The photoresist coated wafer is then patterned via a direct-write photolithography machine (MicroWrite ML3 Pro, Durham Magneto Optics Ltd) exposing the desired pattern to UV light (5000mJ/cm^2) (Fig. S1c). The exposed photoresist coated wafer is then post-exposure baked for 2 minutes at 95°C (Fig. S1d). After post-exposure bake the un-reacted photoresist is removed by developing the wafer via submersion in propylene glycol methyl ether acetate (PGMEA) for 2 minutes (Fig. S1e), then rinsed with fresh PGMEA for a few seconds, followed by rinsing with IPA and dried with compressed nitrogen. The lattices were designed with parameters h = 100 μm, l = 50 μm and t = 10 μm. Once produced, the lattices were characterized using the software imageJ. Five

measurements of h, l and t were taken for each auxetic rotation angle, α, between 25° to 50° to give the average geometrical parameters of the sample as $h = 103.8 \pm 1.5$ μm, $l = 48.8 \pm 1.0$ μm and $t = 13.9 \pm 1.1$ μm. The measured values were then used in the analytical model to predict the Cassie angle as a function of the auxetic rotation angle.

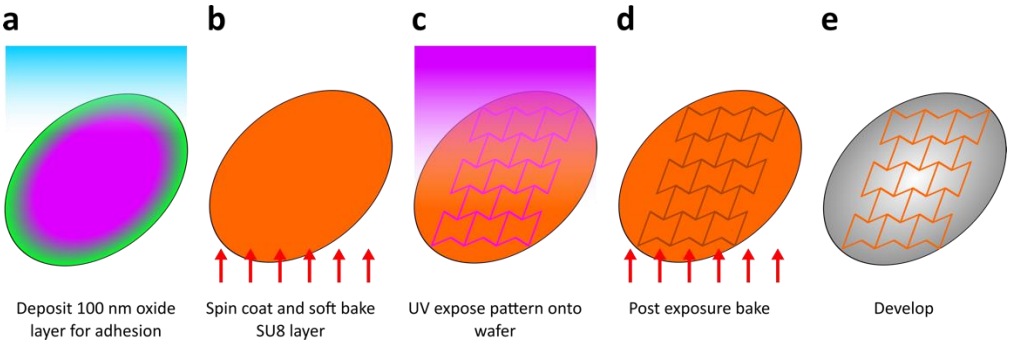

Supplementary Figure S1. Fabrication Process of SU-8 Based Physical Model for an Auxetic Bow-Tie Lattice. a, Silicon wafer with deposition of 100 nm oxide layer for improved adhesion. **b**, Spin coat and soft bake SU8 layer. **c**, UV expose pattern onto resist using direct-write photolithography. **d**, Post exposure bake. **e**, Develop to leave only auxetic bow-tie physical model pattern.

Fabrication of Auxetic Bow-Tie Lattice Membranes.

Typically, micro-patterning of PDMS is achieved by creating a 'stamp' out of SU-8 photoresist[1]. This usually creates a micron-scale pattern on the top surface of a millimetre-scale bulk of PDMS. The bulk PDMS aids the lift-off from the SU-8 mould. To observe auxetic behaviour, the pattern needs to go through the entire material, not just the top surface, this adds an additional challenge in releasing the PDMS from the mould. Dissolving the mould allows release of the PDMS mesh without damaging the complex shapes of the auxetic network. SPR220-7 is a positive photoresist which is dissolvable in acetone, making it a good candidate for a dissolvable mould. SPR220-7 typically allows the creation on ~7 μm thick films. In order to make thicker auxetic networks a method of layering successive thin films of SPR220-7 was achieved by following a modified methodology adapted from Koukharenko *et al.*[2]

First the wafer is treated with hexamethyldisilazane (HMDS) for 10 minutes by keeping the wafer in a closed container with an open vial containing 2-3 drops of HMDS. Once treated, SPR220-7 is poured onto the wafer in a spin coater covering approximately 50% of the wafer. The wafer is then spin coated for: 2 min at 350 rpm with 100 rpm s^{-1} acceleration; then 20 s at 1000 rpm with 100 rpm s^{-1} acceleration. This is then placed on a hotplate for 1 min at 90°C. A second layer is applied with the same spin-coater and hotplate parameters. The wafer is then placed in an oven (Tannay Jr) for 55 min at 90°C. For the third and final coat, once again the same spin-coater and hotplate parameters are used. This time the wafer is placed in the oven for 90 min at 90℃ (Fig. S2a).

The photoresist coated wafer is then patterned *via* direct-write photolithography (MicroWrite ML3 Pro, Durham Magneto Optics Ltd) exposing the desired pattern to UV light, 358 nm wavelength UV light at 1800 mJ cm^{-3} exposure dose. Instead of a typical post exposure bake, the wafer is left for 24 h after exposure to allow the UV light to break down the photoresist. Early development tests showed a post exposure bake would cause unwanted bubbles in the exposed areas, damaging the features of the mould. The wafer is developed using MF-24A with 15 min development time (Fig. S2b).

PDMS is prepared a 5:1 ratio of polymer to cross-linker to improve rigidity over standard 10:1 ratios[3]. The PDMS is placed in a vacuum desiccator for 30 min before use to remove any bubbles created mixing the polymer and cross-linker. The PDMS is poured onto the wafer covering approximately 50% of the wafer, then spun for 1 min at 6000 rpm. This is then cured in the oven for 60 min at 90℃ (Fig. S2c).

To ensure the PDMS rests inside the mould without laying over the top of the features, the wafer is briefly placed in a RIE (JLS Etcher) 15 minutes at 200 W RF power with 60 sccm CF_4 and 15 sccm O_2. This etches the PDMS down, removing any excess on top of the mould (Fig. S2d). After etching the PDMS can be removed from the mould by submersion into acetone (Fig. S2e). The membranes are quickly removed to avoid swelling of the PDMS in the acetone and placed into DI water, here they rest between the water/air interface where they can be removed and placed into the strain apparatus using a 3D printed membrane handling tool (Fig. S3a).

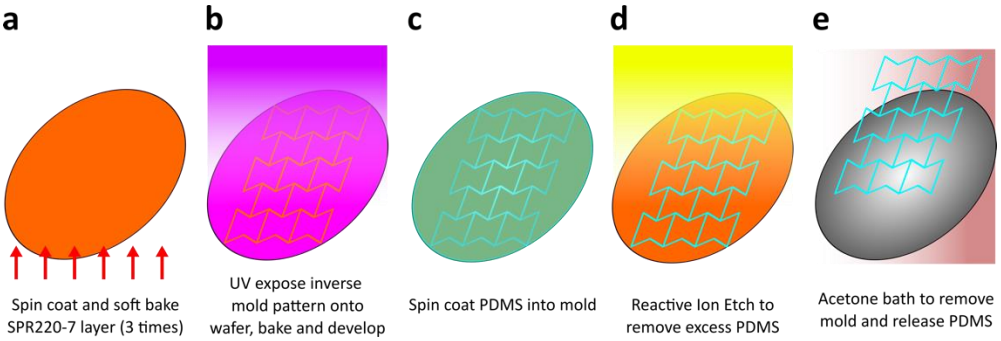

Supplementary Figure S2. Fabrication Process of Auxetic Bow-Tie Lattice Membranes. a, Spin coat 3 successive layers of SPR 220-7 to create a thick ~50 um layer. **b**, UV expose inverse bow-tie pattern to create a negative mould. **c**, Spin coat PDMS into mould. **d**, Shed excess PDMS using reactive ion etching. **e**, Release PDMS membrane by dissolving SPR220-7 mould in acetone.

Hydrophobic Coating of Membranes and SU8-Based Physical Model.

To achieve low contact-line pinning and hydrophobic properties, samples were coated with a polymer brush Slippery Omiphobic Covalently Attached Liquid (SOCAL) layer.[4] First, a thin glass-like layer was added to the surface by spin coating (750 rpm for 40 s) sigmacote (Sigma Aldrich) onto the SU8 structured surface. The sigmacote was left to dry overnight before applying the SOCAL layer. SOCAL was then applied using the optimized method developed by Armstrong *et al.* [5] The wafer was treated with an air plasma at 30% power, 20 minutes and 15 sccm (Henniker HPT-200) to add OH radicals to the glass surface. The wafer was then dipped into a reactive solution of IPA, dimethyldimethoxysilane (Sigma Aldrich), and sulphuric acid (Fisher Chemical; 90, 9, and 1%wt.) for 10 s, and then slowly withdrawn. The wafer is then placed in a bespoke humidity-controlled environment at 60% Relative Humidity and room temperature (18 – 22 C) for 20 minutes. During this step, an acid-catalyzed graft polycondensation of dimethyldimethoxysilane creates a homogeneous layer of PDMS chains grafted to the surface. Any unreacted solution is then rinsed off with IPA, Toluene and DI water to complete the process. The resulting coating exhibits low contact angle hysteresis for sessile droplets (see main text), with higher levels of hysteresis occurring when the plasma intensity and duration are sub-optimal.

To make PDMS membranes superhydrophobic, a commercial spray coating is used (GLACO Mirror Coat, Nippon Shine). PDMS membranes held on a 3D printed membrane handling tool are sprayed from 20 cm distance. Excess liquid on the handling tool is removed via blotting with a Whatman lens tissue to prevent the membrane from migrating along the tool. The membrane is left to air dry for 30 minutes. This coating process is then repeated 3 times to ensure the coating is sufficient to make the surface superhydrophobic.

Strain Measurements on Membranes.

A bespoke strain apparatus was created using two motorized linear stages (MT1-Z8, Thorlabs) controlled *via* software to adjust displacement of the motor position. To load the membrane, the 3D printed tool (Fig. S3a) is attached across the linear stages with additional 3d printed clamps over the top of the membranes (Fig. S3b). The membrane secured to either motorized stage. The supporting center of the 3D printed tool is cut at the point they join the linear stages to allow the membrane to be suspended (Fig. S3c). Finally, the stages are moved apart until the membrane is no longer sagging but with care to not induce a strain (Fig. S3d). This displacement of the linear stages is taken as zero strain. Further displacement of the stage positions inducing a strain in the membrane. Cameras are positioned to the side and underneath of the membrane to capture side view shadowgraph images of droplets on the membranes under varying strain and capture a bottom view of the membrane lattice changes under strain (Fig. S3 b-d). The images of the membrane are analyzed using open-source software Image-J, measuring deformation in the lattice structure as a function of strain. A 5x5 network of unit cells in the center of the membrane was selected. The membrane was filmed under strain and 5 frames were selected at random, with the first one being at zero strain. The length of the network of unit cells along both vertical and horizontal axes for each frame was measured. Total strain along both these directions was calculated using $\varepsilon_{i\_total} = \frac{l_i - l_i^0}{l_i^0}$ where ε_{i_total} is the total strain along direction i, l_i is length of the network along i, and l_i^0 is length of the network at zero strain along i. True strain was then calculated using $\varepsilon_{i\_true} = \ln\left(\frac{l_i}{l_i^0}\right)$ and ε_{1_true}(i.e. true transverse strain) was plotted against

ε_{2_true} (i.e. true loading strain) to determine instantaneous Poisson's ratio ν_{21} for each image from the slope of the graph.

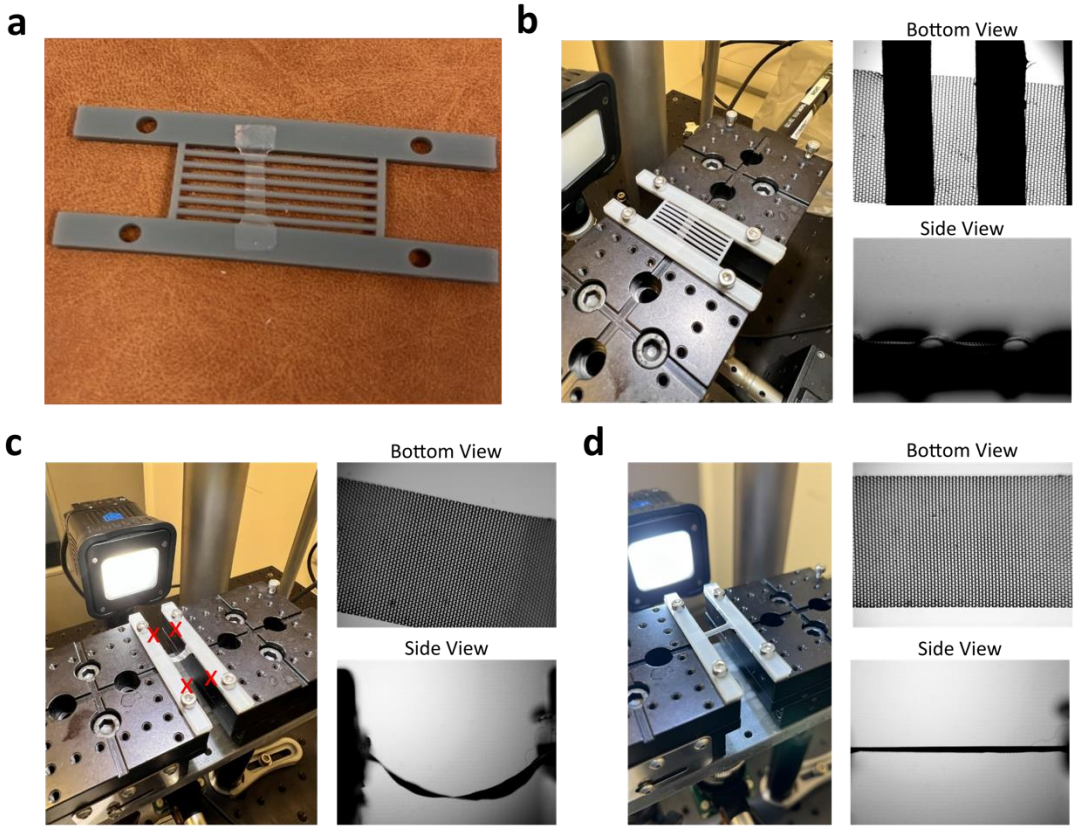

Supplementary Figure S3. Loading of Strain Measurement Apparatus. a, PDMS auxetic bow-tie lattice membrane held on bespoke 3D printed membrane handling tool. **b**, Membrane handling tool attached across two motorized linear stages. **c**, Center support clipped out of membrane handling tool at points denoted by red "X" symbols. **d**, Suspended membrane held at zero strain without sagging.

Contact Angle Measurements.

Side profile images of droplets are taken using shadowgraphy technique on a bespoke goniometer to measure static contact-angle and contact-angle hysteresis of the SU8-based physical model surface. A Microfluidic syringe pump (Exigo, Cellix) is held vertically on a high load vertical stage (VAP10/M, Thorlabs) (Fig S4a) above a triple-axis xyz micron-adjustment stage (PT3/M, Thorlabs) (Fig S4d). This allows precise dosing and placement of droplets onto

the surface. A camera and a small-aperture spotlight (Lumecube 2.0, Lumecube) are placed either side of the droplet to capture images and video sequences (Fig. S4b,c) respectively.

For static contact-angle measurements on the SU8 based physical model, 1.0 ± μL de-ionized water (18.2 MΩ·cm ultrapure type 1) is dispensed and suspended from a flat tipped needle (32 gauge, 0.23 ± 0.01 mm). The suspended droplet is gently lowered to the surface until it attaches to the surface. An image of the droplet profile is taken shortly after touch down on the surface. The static-contact angle is then measured using a 3rd degree polynomial fit of the tangent between the contour of the droplet and the base diameter from the image using open-source droplet shape analysis software (pyDSA).[6]

For static contact-angle measurements on the fluorosilanized PDMS auxetic bow-tie lattice membranes at different strains 1.0 ± 0.02 μL de-ionized water (18.2 MΩ cm ultrapure type 1) is dispensed using a variable volume manual pipette. This is gently lowered onto the surface by hand. An image of the droplet is then taken immediately after touchdown and analyzed using pyDSA as above. 10 droplets are placed at each strain and to give an average static contact-angle for each engineering strain (Fig. S5).

For contact-angle hysteresis measurements, a video is recorded of a droplet dosing/aspiration sequence at 20 frames per second. A 4.0 μL droplet is placed on the surface; the droplet is allowed to relax for 20 seconds to an equilibrium state; with the needle still placed at the top of the droplet 2.0 μL is then dosed at 6 μL s^{-1} allowing another 20 s before the next step in the sequence; 6 μL is then aspirated from the droplet at -6 μL s^{-1}; care is taken during the aspiration to not withdraw so much liquid that the droplet is removed from the surfaces before a receding contact-angle is observed. As previous, pyDSA is used to analyze the droplet contact-angle, throughout the video sequence. The advancing angle is determined as the contact-angle the droplet makes with the surface instantly before the contact-line begins to move during the dosing procedure. The receding angle is determined as the contact-angle the droplet makes with the surface instantly before the contact line begins to move during the aspiration procedure. The contact-angle hysteresis is then calculated as difference between the advancing and receding angle.

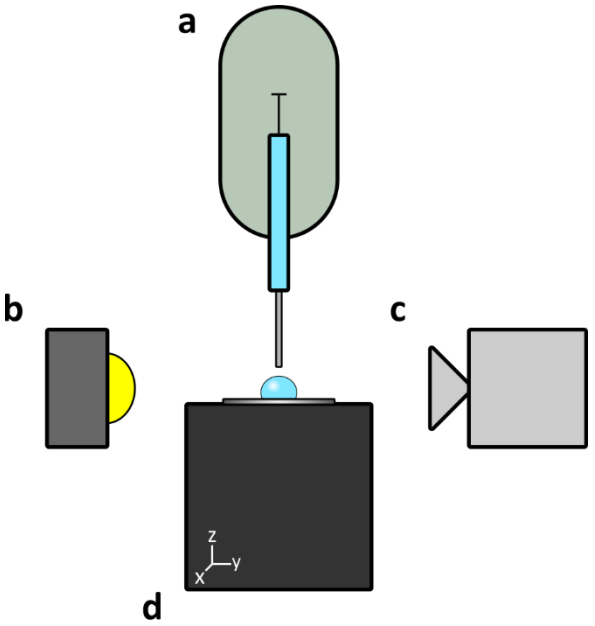

Supplementary Figure S4. Contact Angle Measurement Apparatus. a, Programmable Syringe pump suspended over experiment on a high load vertical stage. **b**, Small aperture backlight. **c**, Macro zoom lens and camera. **d**, Triple axis stage.

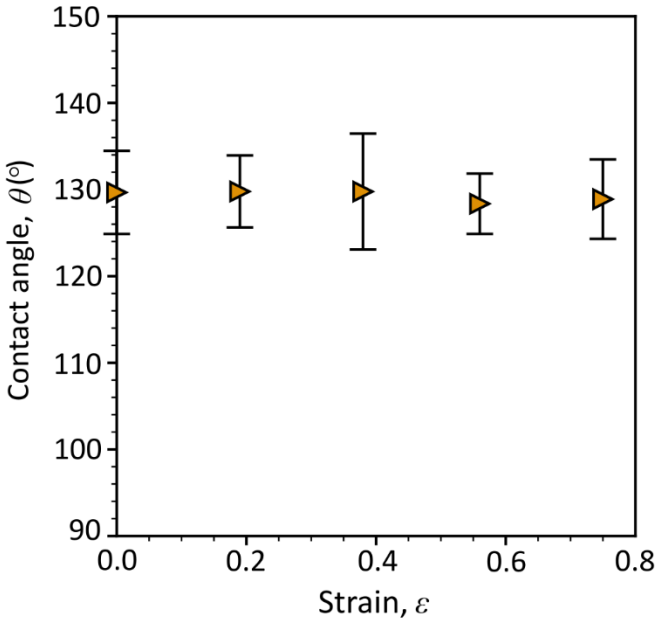

Supplementary Figure S5. Static Contact Angles on Auxetic Bow-Tie Lattice Membranes. Static contact-angle of DI water on fluorosilanized PDMS auxetic bow-tie lattice membranes at

different engineering strains. Images of the membrane at different levels of strain are shown in Fig 4a of the main manuscript.

THEORETICAL ANALYSIS

Model for the Superhydrophobicity of an Auxetic Bow-Tie Lattice.

Supplementary Fig. S6 shows a unit cell of a conventional honeycomb, represented by the dashed red rectangle. Analytical expressions for the projected lengths X_1 and X_2 of the unit cell are developed by representing these distances with respect to the variable parameter, honeycomb angle, α.

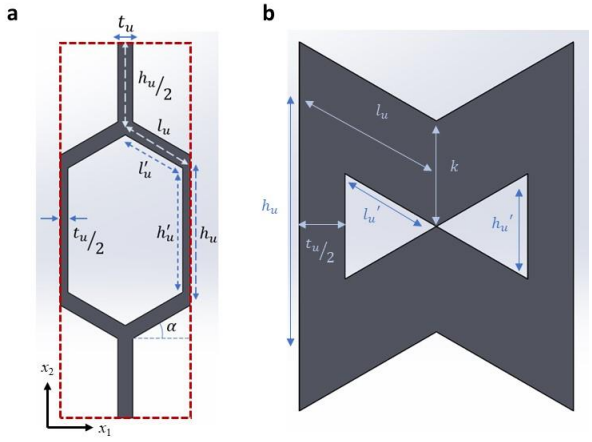

Supplementary Figure S6. Geometry of a Conventional Honeycomb. a, Schematic of the parameterization of the unit cell. Negative values of the rotation angle, α, indicate a clockwise rotation giving an auxetic lattice and positive values indicate an anticlockwise rotation giving a conventional honeycomb. **b**, Maximum thickness of the diagonal rib, l_u' when considering all other parameters

The length of the unit cell along x_1 is,

$$X_1 = 2\, l_u \cos\alpha \qquad \text{(S-e1)}$$

and the length of the unit cell along x_2 is,

$$X_2 = 2\,(h_u + l_u \sin\alpha) \qquad \text{(S-e2)}$$

The area of the unit cell, $A_{\text{cell}}=X_1X_2$, is

$$A_{\text{cell}} = 4l_u \cos\alpha\,(h_u + l_u \sin\alpha) \qquad \text{(S-e3)}$$

Positive α corresponds to an anti-clockwise angle with respect to the horizontal axis, x_1, for the rib shown in the conventional honeycomb (Fig. S6a), and a clockwise, and thus negative, angle

for re-entrant (auxetic) honeycomb geometries. Thus, the rotation angle α determines whether the unit cell is auxetic (positive Poisson's ratio) or conventional (negative Poisson's ratio) and can parameterize the evolution between the two types (Fig. S7).

Parameter	Symbol	Value
Honeycomb angle	α	-55° to 84°
Mesh depth	d_u	5 units
Rib thickness	t_u	1 unit
Rib height	h_u	10 units
Rib length	l_u	5 units

Supplementary Table 1. Table of Standard Honeycomb Parameters.

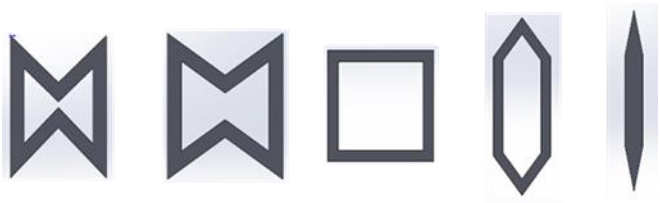

Supplementary Figure S7. Example Evolution of a Unit Cell from Auxetic to Conventional. The evolution is parameterized by the rotation angle α with auxetic shapes corresponding to $-90^o < \alpha < 0$ and conventional shapes corresponding to $0 \leq \alpha < 90^o$. The transition from auxetic to conventional occurs when $\alpha = 0^o$ which corresponds to a rectangular unit cell.

Strain can be calculated using $\Delta X_i/X_i$ where ΔX_i is the difference between the final and initial length of unit cell, and X_i is the initial length, and i represents the direction (either 1 or 2).
The limits for the honeycomb angle are determined by the rib thickness (t_u), height (h_u), and length (l_u). The inner vertical rib height, h'_u, and inner rib length, l'_u, are dependent on t_u , the rib thickness, and honeycomb angle α,

$$h'_u = h_u - \frac{t_u(1-\sin\alpha)}{\cos\alpha} \quad \text{(S-e4)}$$

$$l'_u = l_u - \frac{t_u}{2\cos\alpha} \quad \text{(S-e5)}$$

The Cassie-Baxter state is when a droplet remains in a suspended state, bridging between the gaps (or pores) on the surface of a material. It remains in contact with the solid surface area. A simplifying assumption is to ignore any meniscus in the pore area and assume the liquid-vapor interface remains flat.

The pore area within the unit cell in Fig. 6a is given by,

$$A_{\text{pore}} = 4l'_u \cos\alpha \,(h'_u + l'_u \sin\alpha) \tag{S-e6}$$

From eq. S-e4 and eq. S-e5,

$$A_{\text{pore}} = 4\,\cos\alpha \left(l_u - \frac{t_u}{2\cos\alpha}\right)\left[\left(h_u - \frac{t_u(1-\sin\alpha)}{\cos\alpha}\right) + \left(l_u - \frac{t_u}{2\cos\alpha}\right)\sin\alpha\right] \tag{S-e7}$$

The pore surface fraction, is the ratio of the pore area to the unit-cell area, and is 1 minus the Cassie solid surface fraction, f_s,

$$1 - f_s = \frac{\left(l_u - \frac{t_u}{2\cos\alpha}\right)\left[\left(h_u - \frac{t_u(1-\sin\alpha)}{\cos\alpha}\right) + \left(l_u - \frac{t_u}{2\cos\alpha}\right)\sin\alpha\right]}{l_u(h_u + l_u\sin\alpha)} \tag{S-e8}$$

The Cassie solid surface fraction is the ratio of solid area to the unit-cell area,

$$f_s = 1 - \frac{\left(l_u - \frac{t_u}{2\cos\alpha}\right)\left[\left(h_u - \frac{t_u(1-\sin\alpha)}{\cos\alpha}\right) + \left(l_u - \frac{t_u}{2\cos\alpha}\right)\sin\alpha\right]}{l_u(h_u + l_u\sin\alpha)} \tag{S-e9}$$

The Cassie-Baxter contact angle, θ_{CB}, can be calculated from the weighted average on the solid and air fractions[7],

$$\cos\theta_{\text{CB}} = f_s\,\cos\theta_{\text{S}} - (1 - f_s) \tag{S-e10}$$

where θ_{S} is the contact angle of a droplet on the material of solid and $\cos\theta_{\text{A}}$=-1 because θ_{A}=180$^{\text{o}}$ for air.

Although the honeycomb angle may vary from −90° to 90°, the added thickness, t_u, imposes limits on those extremes. The Cassie solid surface fraction, f_s, starts close to unity and decreases as the diagonal ribs of the honeycomb rotate and cause expansion in the system, creating more pore area. With increasing strain, the auxetic honeycomb opens up reaching a honeycomb angle value of 0°, resembling a rectangle. Under continued strain, the system enters a positive Poisson's ratio regime and starts closing transversely again as the honeycomb ribs rotate and now shorten the length X_1 instead of expanding. Once α reaches its maximum limit, the system reaches a Cassie solid surface fraction close to 1 and is (almost) a complete solid surface.

The effect of rib thickness, t_u, on the Cassie-Baxter angle can be studied by varying it from its minimum thickness of 0 units to its maximum thickness when opposing apexes meet and divide the pore in a unit cell into two distinct parts (Fig. 6b). The maximum thickness of the diagonal rib, l_u, is given by,

$$k = \frac{t_{l_u\_max}}{\cos\alpha} \quad \text{(S-e11)}$$

and

$$k = h_u + 2l_u \sin\alpha \quad \text{(S-e12)}$$

which implies,

$$t_{l_u\_max} = \cos\alpha\,(h_u + 2l_u \sin\alpha) \quad \text{(S-e13)}$$

The maximum thickness of vertical rib is given by,

$$t_{h_u\_max} = 2\,l_u \cos\alpha \quad \text{(S-e14)}$$

Resultant values from eq. S-e12 and eq. S-e13 are compared, and the lowest of the two represent maximum rib thickness, t_u, in honeycomb geometries.

The range of thickness that can be achieved in honeycombs is higher for conventional systems when compared to auxetic ones as the re-entrant structure restricts the maximum allowable thickness. This means that conventional honeycombs can achieve a Cassie solid surface fraction of ~1, i.e. a complete solid, whereas this is not possible for auxetic honeycombs. For a given rib thickness and magnitude of honeycomb angle, $|\alpha|$, Cassie Baxter contact angles are always greater in conventional honeycombs than auxetics.

For example, assuming as 2:1 ratio of rib height to rib length of a honeycomb with a solid material contact angle of θ_S =105^o and rib thickness, t_u=2.5 units, a honeycomb angle of α=-30^o results in a Cassie Baxter contact angle of θ_{CB}=120^o, however its conventional counterpart of α =+30^o honeycomb angle results in a Cassie-Baxter angle of θ_{CB}=140^o. The Cassie-Baxter solid surface fraction for conventional honeycombs is always less than that of its auxetic counterpart, i.e. honeycombs with an angle of α =30^o/45^o/60^o have less solid-to-unit-cell-area compared to auxetic honeycombs with angles of α =-30^o/-45^o/-60^o, respectively. The higher amounts of solid in auxetic honeycombs thus results in lower Cassie-Baxter contact angles.

Theoretical Analysis of Surface area vs Poisson's ratio

Consider a rectangular material of dimensions X and Y, and surface area

$$A = XY. \quad \text{(S-e15)}$$

We now consider an infinitesimal strain ε_y (applicable to both linear and non-linear responses) along the y direction:

$$d\varepsilon_y = \frac{dY}{Y}. \quad \text{(S-e15)}$$

The corresponding infinitesimal strain along x direction, ε_x, obeys

$$d\varepsilon_x = \frac{dX}{X}. \quad \text{(S-e16)}$$

Hence, the Poisson's ratio, ν_{yx}, is

$$\nu_{yx} = -\frac{d\varepsilon_x}{d\varepsilon_y}, \quad \text{(S-e17)}$$

which yields

$$d\varepsilon_x = -\nu_{yx} d\varepsilon_y. \quad \text{(S-e18)}$$

Let us now consider the change in surface area with displacement along y, i.e.,

$$\frac{dA}{dY} = X + Y\frac{dX}{dY} = X\left(1 + \frac{Y}{X}\frac{dX}{dY}\right) = X\left(1 + \frac{d\varepsilon_x}{d\varepsilon_y}\right) = X(1 - \nu_{yx}). \quad \text{(S-e19)}$$

For positive (extension) change in Y, the surface area increases when $\nu_{yx} < +1$, and decreases when $\nu_{yx} > +1$.

The rate of change of surface area with strain is given by

$$\frac{dA}{dY}Y = \frac{dA}{d\varepsilon_y} = XY(1 - \nu_{yx}) = A(1 - \nu_{yx}). \quad \text{(S-e20)}$$

For positive (extension) change in strain along y, the rate of change of surface area with strain increases as ν_{yx} decreases when $\nu_{yx} < +1$, and increases as ν_{yx} increases when $\nu_{yx} > +1$. There is no change in surface area with strain when $\nu_{yx} = +1$.

For a lattice structure with constant solid surface area (A_S) under strain (e.g. a hinging honeycomb), the solid surface fraction, $f_S = A_s/A$, also does not change with strain when $\nu_{yx} = +1$, corresponding to a minimum in the solid fraction vs strain curve.

Note that the range of Poisson's ratio for *isotropic* materials is $-1 < \nu < +0.5$. Hence the decrease in surface area under tension noted above when $\nu_{yx} > +1$ is not possible for isotropic materials, and the minimum in the solid fraction vs strain curve is not observed.
Similarly, the enhanced rate of change of surface area with strain at high magnitude of (negative or positive) Poisson's ratio requires the material to be *anisotropic*.

Video Auxetic Bow-tie Membrane Stretching

Supplementary Video SV1. Auxetic Bow-tie Membrane Stretching. Video demonstration of auxetic bow-tie membrane going from unstrained to strained states with unit cell expansion along strain and perpendicular to the strain. Filmed at 10 fps, playback at 30 fps. Horizontal ribs of unit cell are 100 μm for an indication of scale.

Video of Attempted deposition of Droplet onto a Superhydrophobic Coated Membrane

Supplementary Video SV2. Attempted Deposition of Droplet onto Superhydrophobic Coated Membrane. Video demonstration of difficulty to place a 1.0 μL droplet onto superhydrophobic GLACO coated auxetic bow-tie membrane. Filmed and playback at 100 fps. Pipette tip is 0.90 ± 0.05 mm for an indication of scale.

Supplementary References

1. A. Bubendorfer, X. Liu, A. Ellis, V. *Smart Mater. Struct.* **2007,** *16,* 367.
2. E. Koukharenko, M. Kraft, G. J. Ensell, N. Hollinshead, *J. Mater. Sci. Mater. Electron.* **2005,** *16,* 741.
3. R. Seghir, S. Arscott, *Sensors Actuators, A Phys.* **2015,** *230,* 33.
4. L. Wang, T. J. McCarthy, *Angew. Chemie Int. Ed.* **2016,** *55,* 244.
5. S. Armstrong, G. McHale, R. Ledesma-Aguilar, G. G. Wells, *Langmuir* **2019,** *35,* 2989.
6. G. Launay, PyDSA: Drop Shape Analysis in Python, https://framagit.org/gabylaunay/pyDSA_gui, accessed: October **2023**.
7. N. J. Shirtcliffe, G. McHale, S. Atherton, M. I. Newton, *Adv. Colloid Interface Sci.* **2010,** *161,* 124.